Looking for new synthesis of hydroxyapatite doped with europium

C. S. CIOBANU[a,b], E. ANDRONESCU[a], B. S. VASILE[a], C. M. VALSANGIACOM[b], R. V. GHITA[b], D. PREDOI[b,*]
[a]*University Politehnica of Bucharest, Faculty of Applied Chemistry and Materials Science, Department of Science and Engineering of Oxide Materials and Nanomaterials, 1-7 Polizu Street, P.O. Box 12-134, 011061 Bucharest, Romania*
[b]*National Institute for Physics of Materials, P.O. Box MG 07, Bucharest, Magurele, Romania*

In this work, we synthesized the properties of bioactive nanocrystalline hydroxyapatite (HAp), $Ca_{10}(PO4)_6(OH)_2$ ceramic powder and nanocrystalline HAp doped with europium (III). The europium doped hydroxyapatite with an atomic ratio Eu/(Eu +Ca) between 2% and 20% were synthesized. The structure, morphology and optical properties were characterized by X-ray diffraction (XRD), transmission electron microscopy (TEM), scanning electron microscopy (SEM), X-ray photoelectron spectroscopy (XPS), and Fourier transform infrared spectroscopy (FT-IR). The XRD results reveal that the obtained Eu: HAp shows the characteristic peaks of hydroxyapatite in a hexagonal lattice structure. The results indicated that Eu^{3+} has been successfully doped into the framework of HAp.

(Received September 15, 2010; accepted October 14, 2010)

Keywords: Nanocrystalline hydroxyapatite, Nano-powder, Europium, TEM, XRD, XPS, SEM, FT-IR

1. Introduction

During recent years a lot of efforts have been made for achievement of novel biological luminescent nanocrystals and fluorescent biological labels for medical diagnostics and targeted therapeutics applications [1-12].

Hydroxyapatite, $Ca_{10}(PO_4)_6(OH)_2$ has a hexagonal structure with $P6_3/m$ space group and cell dimensions of a = b = 9.42 Å and c = 6.88 Å [13-14]. Synthetic hydroxyapatite (HAp) ceramic is a preferred material for substitute of filling material for sclerous tissues because of its good biocompatibility and osteoconductivity [15-16]. Moreover, synthesis of ceramics offers several advantages including shorter synthesis time, rapid heating, fast reaction, easy reproducibility, narrow particle distribution, high yield, high purity [17-23]. Because of the high stability and flexibility of the apatitic structure, a great number of substitutions, especially the composites resulting from the cationic substitution are of potential application in the fields of dental and bone pathologies, bioceramics, luminescence, water purification and catalysis [24-29]. Labelling using organic fluorescent molecules is popular in clinical use for some years. In recent time, a lot of inorganic components even nano-particles were suggested to be such candidates [30]. The toxicity of particles used is an extremely important tissue in practical application due to composition and size of nanoparticle. Europium is a luminescent agent with great bio-compatibility and is ideal for implantation and clinical application [31].

This article presents our preliminary research on synthesis and characterization of europium doped nanocrystalline HAp. In this study, europium doped hydroxyapatite with an atomic ratio Eu/(Eu +Ca) between 0%, 2% and 20% were synthesized by mixing $Eu(NO_3)_3{\cdot}6H_2O$, Ca $(NO_3)_2{\cdot}4H_2O$ and $(NH_4)_2HPO_4$ in deionizated water together (Ca/P molar ratio: 1.67 and an atomic ratio Eu/(Eu +Ca) between 0%, 2% and 20%). The structure, morphology, and optical properties of the obtained samples were systematically characterized by X-ray diffraction (XRD), scanning electron microscopy (SEM), transmission electron microscopy (TEM), X-ray photoelectron spectroscopy (XPS), and Fourier transform infrared spectroscopy (FT-IR).

2. Experimental

2.1. Sample preparation

All the reagents for synthesis including ammonium dihydrogen phosphate [$(NH_4)_2HPO_4$], calcium nitrate [Ca $(NO_3)_2{\cdot}4H_2O$], and europium nitrate [$Eu(NO_3)_3{\cdot}6H_2O$] (Alpha Aesare) were purchased without further purification.

Europium-doped hydroxyapatite was obtained at 80^0C. The Eu: $Ca_{10}(PO_4)_6(OH)_2$ (Eu:HAp) was obtained by mixing together $Eu(NO_3)_3{\cdot}6H_2O$, $Ca(NO_3)_2{\cdot}4H_2O$ and $(NH_4)_2HPO_4$ in deionizated water (Ca/P molar ratio: 1.67 and an atomic ratio Eu/(Eu +Ca) between 0%, 2% and 20%) and stirred until a homogeneous solution was formed. The pH was adjusted to 9 using 2M NH_3. The obtained precipitate was then filtered washed several times with deionizated water. The resulting material was dried at 80 ^{o}C for 72h.

2.2. Sample characterization

X-ray diffraction (XRD). The samples were characterized for phase content by X-ray diffraction (XRD) with a Bruker D8-Advance X-ray diffractometer in the scanning range 2θ = 15 – 140 using $CuK_{\alpha 1}$ incident radiation.

Scanning electron microscopy (SEM). The structure and morphology of the samples were studied using a HITACHI S2600N-type scanning electron microscope (SEM), operating at 25kV in vacuum. The SEM studies were performed on powder samples. For the elemental analysis the electron microscope was equipped with an energy dispersive X-ray attachment (EDAX/2001 device).

Transmission electron microscopy (TEM) studies were carried out using a JEOL 200 CX. The specimen for TEM imaging was prepared from the particles suspension in deionized water. A drop of well-dispersed supernatant was placed on a carbon – coated 200 mesh copper grid, followed by drying the sample at ambient conditions before it is attached to the sample holder on the microscope.

FT-IR spectroscopy. The functional groups present in the prepared powder and in the powders calcined at different temperatures were identified by FTIR (Spectrum BX Spectrometer). For this 1% of the powder was mixed and ground with 99% KBr. Tablets of 10 mm diameter for FTIR measurements were prepared by pressing the powder mixture at a load of 5 tons for 2 min and the spectrum was taken in the range of 400 to 4000 cm^{-1} with resolution 4 and 128 times scanning.

X-ray Photoelectron Spectroscopy (XPS) is one of the most powerful techniques for the study of the evidence for successful doping of Eu^{+3} in Eu:HAp. It can be said that the surface sensitivity (typically 40-100 Å) makes this technique ideal for measurements as oxidation states or biomaterials powder. In this analysis we have used a VG ESCA 3 MK II XPS installation ($E_{k\alpha}$=1486.7 eV). The vacuum analysis chamber pressure was p~ 3×10^{-8} torr. The XPS recorded spectrum involved an energy window w=20 eV with the resolution R= 50 eV with 256 recording channels. The XPS spectra were processed using Spectral Data Processor v 2.3 (SDP) software.

3. Results and discussion

3.1. X-ray diffraction

Fig. 1 shows the XRD patterns of pure HAp and Eu:HAp with (Ca+Eu)/P=2% and (Ca+Eu)/P=20%. Fig. 1 (A) shows the typical diffraction peaks of hexagonal $Ca_{10}(PO_4)_6(OH)_2$. The following approximations were done: i. the hydroxylapatite and calcium oxide unit cell structures were restricted, in what concerns: atomic sites, occupancies and temperature factors, to ICSD card no 99358, for hydroxylapatite [32] and to ICSD card no. 90486, for lime [33]; ii. no internal stresses (lattice disorder) were assumed. For (Ca+Eu)/P=20%, the presence of a very broad peak in the region of the highest peak in of note, as it is characteristic of a poorly crystalline phase.

The determination of the average crystallite size by XRD method is based on the Scherrer equation:

$$D_{crystallite} = K\lambda/B\cos\theta$$

where $D_{crystallite}$ is the averaged length of coherence domains (that is of perfectly ordered crystalline domains) taken in the direction normal to the lattice plane that corresponds to the diffraction line taken into account, B is the line broadening due to the small crystallite size, λ is the wavelength of X-rays, θ is the Bragg angle, and K a constant related to crystallite shape and to the definition of B (integral breadth or full width at half maximum). The following results were obtained for the mean crystallite size: D = 18 nm (±0.1) for pure HAp, D = 15 (±0.7) nm for Eu:HAp with (Ca+Eu)/P=2% and D = 12 nm (±0.5) nm for Eu:HAp with (Ca+Eu)/P=20%.

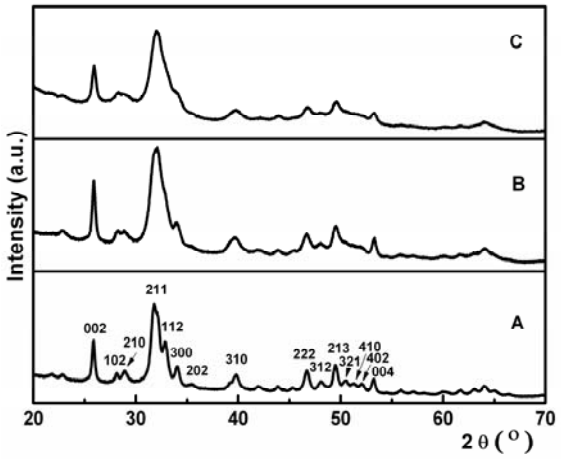

Fig. 1. XRD patterns of pure HAp (A), Eu:HAp with (Ca+Eu)/P=2% (B) and Eu:HAp with (Ca+Eu)/P=20% (C).

3.2. Scanning electron microscopy

The SEM images of pure HAp (Fig. 2A) and Eu:HAp (Fig. 2 B-C) are presented in (Fig. 2A-C). SEM images provide the direct information about the morphology of the as-prepared samples. The results suggest that the doping of Eu^{3+} has an influence on the morphology. The pure HAp powder shows spherical particles. For the Eu:HAp the particles are ellipsoidal. The EDS spectrum (Fig. 2 E-F) of Eu:HAp confirms the presence of calcium (Ca), phosphorus (P), oxygen (O) and europium (Eu) in the Eu:HAp sample.

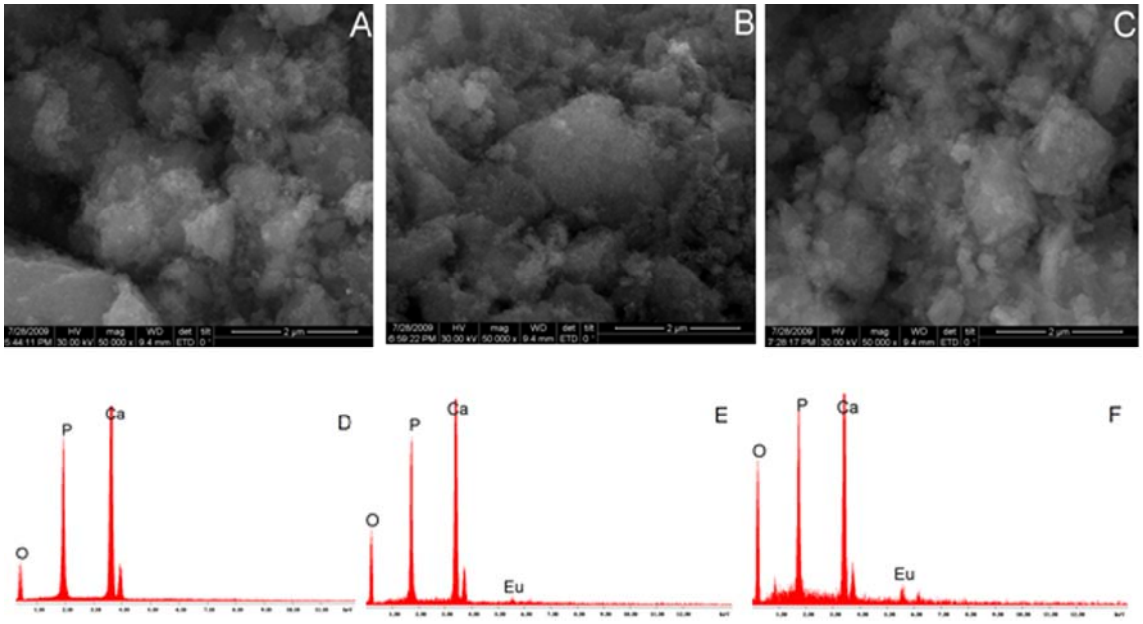

Fig. 2. SEM images of pure Hap (A), Eu:HAp with(Ca+Eu)/P=2% (B) and Eu:HAp with (Ca+Eu)/P=20% (C). EDS spectrum of pure Hap (D), Eu:HAp with(Ca+Eu)/P=2% (E) and Eu:HAp with (Ca+Eu)/P=20% (F).

3.3. Transmission electron microscopy

Fig. 3 exhibits the TEM images of pure HAp (A), Eu:HAp with(Ca+Eu)/P=2% (B) and Eu:HAp with(Ca+Eu)/P=20% (C) with low resolution. It is found that the particles of pure Hap are spherical. On the other hand we can see that the particles of Eu:Hap samples are ellipsoidal. The results are in good agreement with the SEM results, revealing that the doping components have an influence on the surface morphology of the samples.

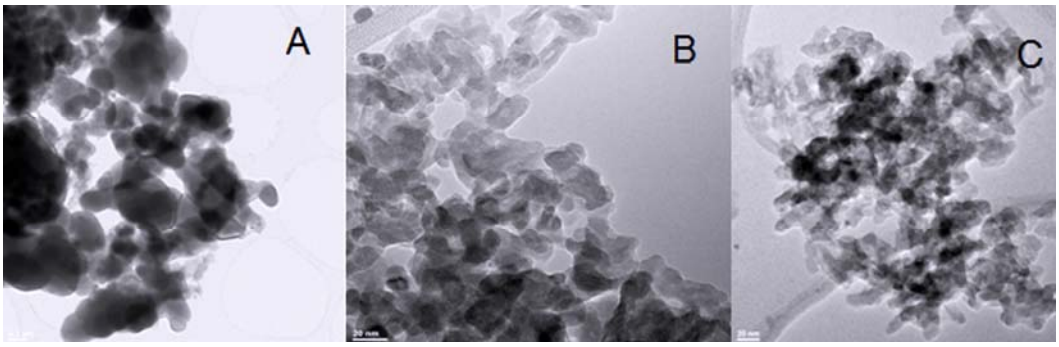

Fig. 3. TEM images of pure Hap (A), Eu:HAp with(Ca+Eu)/P=1% (B) and Eu:HAp with(Ca+Eu)/P=20% (C).

3.4. FT-IR spectroscopy

FT_IR spectra of pure HAp (A), Eu:HAp with (Ca+Eu)/P=2% (B) and Eu:HAp with(Ca+Eu)/P=20% (C) are presented in Fig. 4.

The peaks of 1032 cm^{-1} correspond to the asymmetric stretching vibration of PO_3^{-4}, and the peaks of 600, 560 cm^{-1} in pure HAp (Fig. 4A) and the peaks of 604, 563 cm^{-1} in Fig. 4 (B-C) correspond to the bending vibration [34-36]. The peaks of 3452 cm^{-1} in Fig. 4A indicate the samples contained a little OH. Similarly, the peaks of 1419 and 3456 cm^{-1} (Fig. 2B) and 3465 cm^{-1} (Fig. 4C) indicate that the samples contained a small amount of CO_2^{-3} and OH, respectively.

In Fig. 1A, the wave number of OH in pure HAp are 3452 and 1630 cm^{-1}, and the wave number of OH in Eu:HAp with (Ca+Eu)/P=2% are 3456 and 1638 cm^{-1} (Fig. 4B), while in Eu:HAp with (Ca+Eu)/P=20% are 3465 and 1644 cm^{-1} (Fig. 4C). In good according with [37] we can see that the wave number of the OH band increases with the radii of cations of hydroxyapatite owing to the increase in the hydrogen bond distance OH.

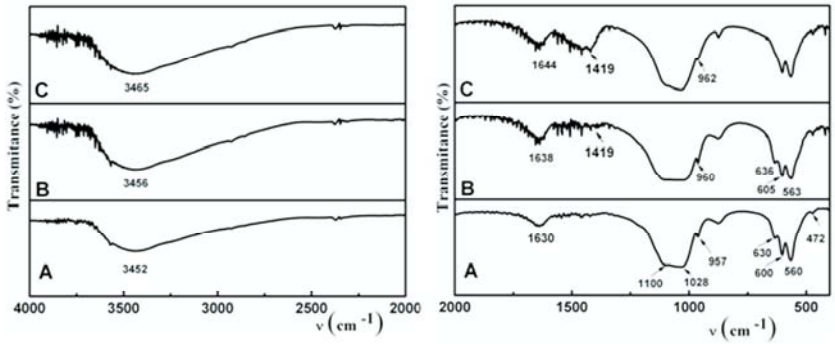

Fig. 4. FT_IR spectra of pure HAp (A), Eu:HAp with (Ca+Eu)/P=2% (B) and Eu:HAp with (Ca+Eu)/P=20% (C) (in the region 4000-2000 cm^{-1} (left) and 2000-400 cm^{-1} (right)).

3.5. X-ray photoelectron spectroscopy

XPS technique has been tested as a powerful tool for qualitatively determination of surface composition of one material. The general XPS spectra for undoped pure HAp are presented in Fig. 5A. The XPS spectrum of pure HAp shows the binding energy of Ca (2p, 347.10 eV), O (1s, 531 eV) and P (2p, 133.8 eV) respectively. The Ca 2p signal present the peaks $2p^{3/2}$ 347.13eV related to Ca-O bond and $2p^{1/2}$ at 350.67 present in complex combinations as HAp. The reference line of C 1s specified for C-C bond at the energy 285eV is used as calibration for the present spectra. As a general observation the ratio Ca/P is nearly stoichiometric.

The XPS spectrum of Eu :Hap with (Ca+Eu)/P=2% and with (Ca+Eu)/P=20% (Fig. 5B-C) shows the binding energy of Eu (3d, 1132.3 eV), Ca (2p, 347.5 eV), O (1s, 532.1 eV) and P(2p, 133.9 eV), respectively. By combination of previous XPS results, it can be deduced that these signals can be assigned to Eu:HAp. XPS results provide the additional evidence for the successful doping of Eu^{3+} in Eu:HAp.

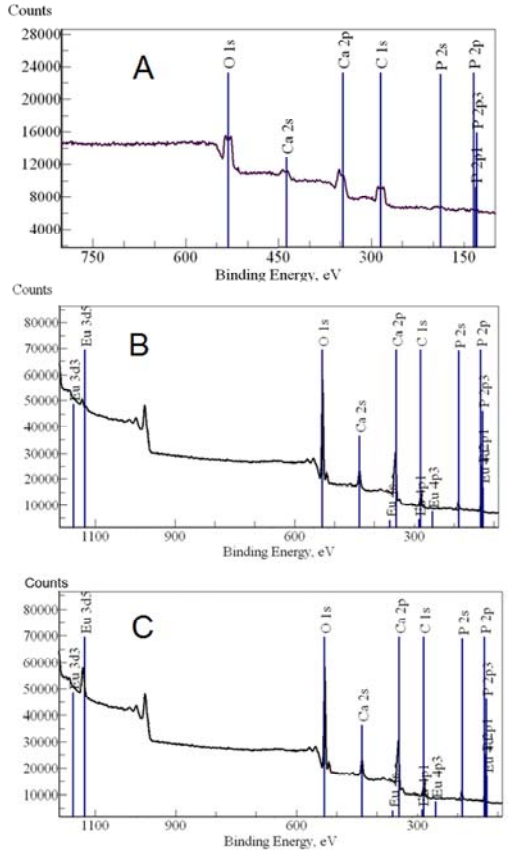

Fig. 5. XPS spectrum of the pure HAp (A), Eu:HAp with (Ca+Eu)/P=2% (B) and Eu:HAp with (Ca+Eu)/P=20% (C).

4. Conclusions

The europium-doped HAp were synthesized at 80 ^{0}C by co-precipitating from a mixture of Ca^{2+} and Eu^{3+} ions by phosphate ions in water medium. The preliminary DRX studies have shown that Eu^{3+} has been successfully doped into HAp. The results reveal that the obtained pure HAp and Eu:HAp particles are well assigned to the hexagonal lattice structure of the hydroxyapatite phase. The europium-doped HAp show a potential application in various fields based on their nano-sized and luminescent properties.

Acknowledgements

This work was financially supported by Science and Technology Ministry of Romania (PNCDI II 71-097/2007, Core Program contract PN09-45 and POSDRU ID7713).

References

[1] K. E. Uhrich, S. M. Cannizzaro, R. S. Langer, K. M. Shakesheff, Che. Rev. **99**, 3181 (1999).
[2] L. Di Silvio, W. Bonfield, J. Mater. Sci. Mater. Med. **10**, 653 (1999).
[3] R. Cortesi, C. Nasturzzi, S. S. Davis, Biomaterials **19**, 1641 (1998).
[4] R. Narayani, K. Panduranga, Int. J. Pharm. **142**, 25 (1996).
[5] E. Esposito, R. Cortesi, C. Nasturzzi, Biomaterials **17**, 2000 (1966).
[6] T. Chandy, C. T. Sharma, Biomaterials **17**, 61 (1996).
[7] W. Paul, C. T. Sharma, J. Mater. Sci. Mater. Med. **10**, 383 (1999).
[8] M. Itokazu, W. Yang, T. Aoki, A. Ohara, Biomaterials **19**, 817, (1998).
[9] A. Almirall, G. Larrecq, J. A. A. Delgado, Biomaterials **17**, 3671 (2004).
[10] J. E. Barralet, K. J. Lilley, L. M. Grover, D. F. Farrar, C. Ansell, U. Gbureck, J. Mater. Sci. Mater. Med. **15**, 407 (2004).
[11] A. C. Queiroz, J. D. Santos, F. J. Monteiro, Bioceramics **17**, 407 (2005).
[12] M. A. Rauschmann, T. A. Wichelhaus, V. Stirnal, E. Dingeldein, L. Zichner, R. Schnettler, V. Alt, Biomaterials **26**, 2677 (2005).
[13] K. D. Groot, C. P. A. T. Klein, J. G. C. Wolke, J. M. A. Blieck-Hogervorst, in: T. Yamamuro, L. L. Hench, J. Wilson (Eds.), Handbook of Bioactive Ceramics, **2**, (CRC Press, Boca Raton, FL, 1990).
[14] S. J. Kalita, A.Bhardwaj, H. A. Bhatt, Materials Science and Engineering: C **27**, 441 (2007).
[15] S. P. Li, Introduction of Biomedical Materials, (Wuhan: Wuhan University of Technology Press, 2000 (in Chinese)).
[16] A. Hideki, Hydroxyapatite, Tokyo: Japanese Association of Apatite Science, 1998.
[17] J. K. Han, H. Y. Song, F. Saito, B. T. Lee, Materials Chemistry and Physics **99**, 235 (2006).
[18] S. Katakam, D. Siva Rama Krishna, T. S. Sampath Kumar, Materials Letters **57**, 2716 (2003).
[19] I. Manjubala, M. Sivakumar, Materials Chemistry and Physics **71**, 272 (2001).
[20] S. Meejoo, W. Maneeprakorn, P. Winotai, Thermochimica Acta **447**, 115 (2006).
[21] P. Parhi, A. Ramanan, A. R. Ray, Materials Letters **58**, 3610 (2004).
[22] A. Siddharthan, S. K. Seshadri, T. S. S. Kumar, Scripta Materialia **55**, 175 (2006).
[23] S. Vijayan, H. Varma, Materials Letters **56**, 827 (2002).
[24] Y. Matsumura, S. Sugiyama, H. J. B. Hayashi, J. B. Moffat, J. Solid State Chem. **114**, 138 (1995).
[25] E. Boanini, P. Torricelli, M. Gazzano, R. Giardinob, A. Bigi, Biomaterials **29**, 790, (2008)
[26] X. Chen, T. Wu, Q. Wang, J. W. Shen, Biomaterials **29**, 2423 (2008).
[27] J. K. Liu, Q. S. Wu, Y. P. Ding, Eur. J. Inorg. Chem. 4145 (2005).
[28] S. Sebti, R. Tahir, R. Nazih, A. Saber, S. Boulaajaj, Appl. Catal. A Gen. **228**, 155 (2002).
[29] W. Andreoni, D. Scharf, P. Giannozzi, Chemical Physics Letters **173**, 449 (1990).
[30] A. Doat, F. Pellé, A. Lebugle, Journal of Solid State Chemistry. **178**, 2354 (2005).
[31] A. Doat, M. Fanjul, F. Pellé, E. Hollande, A. Lebugle, Biomaterials **24**, 3365 (2003).
[32] L. M. Rodriguez-Lorenzo, J. N. Hart, K. A. Gross, J. Phys. Chem. B **107**, 8316 (2003).
[33] R. Ganguly, V. Siruguri, I. K. Gopalakrishnan, J. V. Yakhmi, Journal of Physics: Condensed Matter. **12**, 1683 (2000).
[34] D. Predoi, R. A. Vatasescxu-Balcan, I. Pasuk, R. Trusca, M. Costache, J. Optoelectron. Adv. Mater. **10**, 2151 (2008).
[35] D. Predoi, R. V. Ghita, F. Ungureanu, C. C. Negrila, R. A. Vatasescu-Balcan, M. Costache, J. Optoelectron. Adv. Mater. **9**, 3827 (2007).
[36] D. Predoi, M. Barsan, E. Andronescu, R. A. Vatasescu-Balcan, M. Costache, J. Optoelectron. Adv. Mater. **9**, 3609 (2007).
[37] X. Y Cao, F. Wen, W. Bian, Y. Cao, S. J. Pang, W. K. Zhang, Front. Mater. Sci. China **3**, 255 (2009).

*Corresponding author: dpredoi68@gmail.com